The Aging Behavior of Types 308 and 308CRE Stainless Steels and Its Effect on Mechanical Properties[*]

J. M. Vitek and S. A. David
Oak Ridge National Laboratory
Metals and Ceramics Division
P. O. Box X
Oak Ridge, Tennessee 37831-6376

ABSTRACT

The aging behavior of types 308 and 308CRE stainless steels has been examined over a range of temperatures (475 - 850°C) for aging times up to 10,000 hours. Both the homogenized and the as-welded initial conditions were studied. At elevated aging temperatures (>550°C), aging of type 308 steel resulted in precipitation of carbides and the transformation of ferrite to sigma phase when ferrite was initially present, or the formation of sigma phase in initially ferrite-free material. The elevated-temperature aging of type 308CRE steel resulted in the precipitation of titanium-rich carbides, nitrides, and sulfides, and the transformation of ferrite to sigma phase. The distribution of precipitates was affected by the initial condition of the materials. The elevated-temperature creep properties, and in particular the improved properties of type 308CRE, were related to the precipitate distribution. For low temperature (<550°C) aging of welded type 308 steel, precipitation of G-phase within the ferrite was observed, as well as the decomposition of ferrite into alpha and alpha prime. With the help of a novel mechanical properties microprobe, which was

capable of determining the hardness of the minor constituent ferrite phase, the hardness behavior as a function of aging could be related to the microstructures. These results are interpreted in terms of the potential susceptibility of these alloys to 475°C embrittlement.

INTRODUCTION

Austenitic stainless steels are commonly used materials for elevated-temperature applications in the chemical and nuclear industries. However, during welding, those alloy types which solidify in the fully austenitic condition, such as Type 310 stainless steel, are subject to hot-cracking. In order to avoid, or at least considerably reduce, the susceptibility of these steels to hot-cracking, austenitic stainless steel weld filler metal compositions are chosen to promote ferrite formation during solidification. Type 308 stainless steel is an example of such a weld filler metal. It has been shown that austenitic stainless steels that solidify as primary ferrite are not prone to hot-cracking [1-8], even though the primary ferrite in these steels may undergo a solid-state transformation during further cooling, resulting in a predominantly austenitic structure with as little as 5 to 10% residual ferrite. Several explanations for the reduced crack susceptibility of such duplex steels have been proposed. These include: (a) the higher solubility of tramp elements in ferrite, which reduces the effects of solute segregation during solidification, (b) the lower coefficient of

thermal expansion and higher specific volume of ferrite which reduces the residual stresses that may develop during solidification and cooling, (c) the increased interfacial surface area which may inhibit the propagation of cracks, and (d) the elimination of solidification boundaries by the transformation of ferrite to austenite during cooling. Although the explanation for the improved hot-cracking resistance is not clear, the beneficial effect of primary ferrite solidification is well accepted.

The microstructures in duplex austenite plus ferrite welds are typically unstable. In Fig. 1, a vertical section of the iron-chromium-nickel ternary phase diagram is presented. For the composition shown by the dashed line, which corresponds roughly to that of Type 308 stainless steel, the ferrite that forms during solidification transforms to austenite at lower temperatures, resulting in a fully austenitic structure in equilibrium below approximately 1200°C (~2200°F). However, at the cooling rates encountered during welding, this solid-state transformation does not proceed to completion, leaving some residual ferrite in the as-welded microstructure. With subsequent exposure to elevated temperatures, either as a result of multi-pass welding or during service, the presence of ferrite leads to an instability in the microstructure. In addition to the ferrite instability, the formation of carbides during aging also takes place over a broad temperature range. The phase stability of type 308 stainless steel, with a particular emphasis on the stability of welded microstructures, has been the subject of an ongoing research program at ORNL over the last several

years.

In addition to aging studies at temperatures above 550°C, work was begun recently on studying the aging behavior of type 308 stainless steel at lower aging temperatures in the range of 400 to 550°C. In this temperature range, the phenomenon of 475°C (885°F) embrittlement is common in ferritic steels. Since the type 308 welds contain ferrite with a composition similar to that of ferritic steels with 100% ferrite, the aging behavior of the duplex steel welds is being investigated to evaluate the susceptibility of these steels to the same embrittlement phenomenon.

It was shown several years ago that minor additions of selected elements, in particular titanium, boron, and phosphorous, result in improved creep properties of the as-welded materials [9-11]. These additions are known as controlled residual element (CRE) additions, and the modified filler metal alloy is known as type 308CRE stainless steel. A plot of creep stress vs creep-rupture time illustrating the significant improvement in creep properties of type 308CRE weld metal, compared to type 308 steel, is given in Fig. 2. Earlier work showed that cracking evident in the gage sections of type 308 creep specimens near the sigma-austenite interfaces was absent in the 308CRE welded creep specimens, even though sigma phase was present in this latter alloy [11]. However, the reason for the absence of cracking and the improved creep behavior of the type 308CRE alloy was not known. As part of the study on the stability of type 308 steels, the aging behavior of types 308 and 308CRE steels has been compared in order to understand and

explain the basis for the improved creep properties in the latter alloy.

The purpose of this paper is to integrate the results from various studies that have been reported separately, and present a unified description of the aging behavior of types 308 and 308CRE steels. Results on low-temperature aging (475°C, 887°F) as well as higher-temperature aging will be presented. Results from aging studies with and without concurrent stress will be described. The phase stability results will be related to the mechanical property behavior of these alloys. Details on specific aspects of the phase stability work are available elsewhere [13-18].

EXPERIMENTAL PROCEDURE

The two alloys used in this study were a commercial grade type 308 stainless steel filler metal and a modified type 308 steel with only a titanium addition (to be referred to as type 308CRE even though additions of boron and phosphorous were not present). The major elemental compositions of the steels in the various conditions evaluated are given in Table 1. Two initial conditions prior to aging were examined: homogenized or as-welded. The homogenized material was produced by arc melting and drop casting 2.5-cm-diam ingots and then swaging the ingots down to 0.95-cm-diam rod, with two intermediate anneals at 1080°C. The final size rod was then homogenized at 1080°C for one hour followed by a water quench. This treatment produced a fully austenitic structure in the type 308 steel, and a duplex

austenite plus approximately 10 % ferrite structure in the type 308CRE steel. Representative micrographs of the homogenized structures are shown in Fig. 3. A range of homogenization treatments were examined in order to try to produce a fully austenitic structure in the type 308CRE steel, but the duplex structure could not be avoided [17].

The as-welded samples were produced by multi-pass welds deposited on a 12.7-mm thick type 304L stainless steel plate containing a single V-groove butt joint. Welds were made using the gas-tungsten-arc (GTA) process. Both welded steels had duplex microstructures consisting of austenite with approximately 10% ferrite. Representative micrographs showing the as-welded structures are given in Fig. 4. The ferrite numbers, determined by magnetic measurements in accordance with standard procedures [19], for the type 308 and 308CRE steels in the as-welded condition were 8.5 and 13.0, respectively.

Aging treatments were carried out on small sections cut from the homogenized or welded material. The samples were encapsulated in quartz tubes that were evacuated and then refilled with a partial pressure of argon. Aging temperatures were 475, 550, 650, 750, and 850°C (877, 1022, 1202, 1382, and 1562 °F) and aging times were up to 10,000h. Creep specimens machined from the homogenized or as-welded material were creep-tested at 16 ksi at 650°C (1202°F) and the microstructures were examined at various stages of the tests, up to rupture. In this way, the effect of stress and deformation could be evaluated.

After aging, the specimens were evaluated by a variety of means. The ferrite content was monitored by measuring the

magnetic permeability with a Magne-Gage instrument. Measurements were made on the same samples before and after aging, and the changes were normalized with respect to the initial ferrite levels. The degree of precipitation was determined as a function of aging by conducting chemical extractions on the samples. Details of these procedures may be found elsewhere [13,20].

Microstructural analysis was performed by a combination of optical metallography, scanning electron microscopy, and transmission electron microscopy. Scanning electron microscopy was performed on the metallographically mounted ruptured specimens. Thin-foil specimens for transmission electron microscopy were made from 3-mm-disks that were electron-discharge machined from wafers sliced from the bulk material. After grinding to a thickness of 0.25 mm, the disks were electrochemically polished and examined in transmission electron microscopes operated at 120 or 200 keV.

Hardness measurements were carried out on the ferrite in the welded type 308 steel aged at 475°C in order to evaluate the effect of low temperature aging on the mechanical properties. Since the ferrite was a minor constituent and present on a very fine scale in the microstructure, conventional microhardness measurements were not appropriate. Instead, a mechanical properties microprobe was utilized, which allowed hardness measurements to be made on a scale of less than 1 micrometer in size. Prior to making the hardness measurements, the samples were electropolished to ensure that any work-hardened layer on the sample surface was removed. Details on this novel method of measuring hardness are provided elsewhere [18,21,22].

RESULTS AND DISCUSSION

Precipitation Behavior

Initially, either in the homogenized or in the as-welded condition, very little precipitate (<0.1 wt %) was present in the type 308 steel. With aging at 650°C and above, abundant precipitation of $M_{23}C_6$ carbide occurred. The precipitation reaction was essentially complete within 10 hours for the initially welded material and within 200 hours for the homogenized condition. The amount of precipitate was related to the carbon content. The homogenized material contained more carbon (0.07 wt %) and therefore more precipitate was found (1 wt %). For the welded samples, with only 0.05 wt % carbon, approximately 0.5 wt % precipitate was detected. Although the type of precipitate formed during aging was similar in the homogenized and welded samples, the distribution of the precipitate was very different. In the homogenized material, precipitation occurred primarily along the austenite grain boundaries, whereas in the welded material, the carbide formation was along the austenite/ferrite interfaces. These differences are illustrated in Fig. 5. The precipitation of carbide was slower at 550°C for material in the welded condition, requiring approximately 100 hours before significant amounts of carbide formed. Very limited precipitation was found after aging homogenized material for up to 1000 hours at 550°C. Aging of welded type 308 stainless steel material at 475°C produced some carbide formation at the austenite/ferrite interfaces, but in addition, precipitation of G-phase within the ferrite was also

detected. This is shown in Fig. 6. G-phase is a silicide based on the stoichiometric formula $Ti_6Ni_{16}Si_7$ [16]. Analytical electron microscopy indicated manganese substituted for the titanium in the aged 308 weld metal.

The precipitation behavior of type 308CRE was quite different. The homogenized 308CRE initially contained approximately 0.4 wt % precipitate in the form of titanium-rich carbides, nitrides, and sulfides. Very little additional precipitate was found upon aging. These precipitates were randomly distributed throughout the microstructure, as shown in Fig. 7. As-welded type 308CRE contained only 0.1 wt % precipitate initially, but additional precipitation to a level of 0.4 wt % took place within 10 hours of aging at 550°C and above. During the early stages of aging of type 308CRE at 550°C and above, G-phase precipitation, similar to that found in type 308 steel aged at 475°C, was found in addition to the titanium-rich precipitates. The G-phase formed along dislocations within the ferrite, as shown in Fig. 8, but with longer aging times the G-phase dissolved. Although this phase did not remain stable during aging for long times at temperatures above 550°C, the appearance of G-phase in the aged type 308CRE and not in the 308 steel indicates that it may have a greater stability in the former alloy.

The G-phase has been found in types CF 8 and CF 8M cast stainless steels, both duplex austenite plus ferrite steels containing approximately 15 to 20% ferrite [23]. The G-phase precipitation was found after long-term, low-temperature aging at 400°C. These results indicate that, in general, G-phase is a

stable precipitate in these alloy types at low temperatures. The kinetics of the precipitation process are slow, with several hundred or thousand hours of aging (depending on the temperature) required before the phase appears.

The presence of stress in the creep specimens did not significantly affect either the amount of precipitate or the distribution of the precipitate particles for either of the two alloys or the two initial conditions. This is illustrated in Fig. 9, which shows the amount of precipitate as a function of aging time for type 308 stainless steel aged at 650°C. The distribution of carbides found in the stressed gage section of the creep specimens was similar to that found in aged-only specimens, as shown in Fig. 10.

Ferrite Stability and the Sigma Phase Transformation

For those alloys that initially contained ferrite (welded 308, and both homogenized and welded 308CRE), limited ferrite dissolution took place during the early stages of aging. The initial shrinkage of ferrite is reflected by an early drop (approximately 30%) in the ferrite content, as illustrated in Fig. 11 for aging at 650°C. The ferrite dissolution led to a recession of the austenite/ferrite interface into the ferrite; a concurrent enrichment in chromium and depletion of nickel in the ferrite took place. This partial dissolution is shown in Fig. 12, where the location of the initial austenite/ferrite interface is marked by the precipitation of carbide. During aging, the ferrite composition approaches a limit, which represents metastable equilibrium between the ferrite and austenite [14].

With further aging, the remaining ferrite undergoes a solid-state transformation into sigma phase, resulting in the eventual total elimination of ferrite (see Fig. 11). The sigma transformation is nucleation controlled [15] and is typically a very sluggish reaction, but with the presence of ferrite, this transformation is accelerated and is nearly complete within 500 hours of aging [13,17]. The kinetics for the sigma transformation are comparable for both the 308 and 308CRE alloys in the welded condition. For the homogenized type 308 steel, which did not contain any ferrite initially, nucleation of sigma phase is retarded and the transformation to sigma phase only begins after several thousand hours of aging [17].

The results of aging studies at 475°C show a quite different behavior with regard to the ferrite stability. No evidence of the transformation of ferrite to sigma phase was found in samples aged 5000 hours. Carbide formation at the austenite/ferrite interface was detected, and some shrinkage of the ferrite similar to that found at higher aging temperatures was found. However, within the ferrite, a fine scale decomposition was detected. Although the scale of the decomposed structure was too fine for compositional analysis, the nature of the decomposition is identical to the decomposition of ferrite into alpha and alpha prime that is found in ferritic steels [24-29]. The alpha and alpha prime are body centered cubic phases that are iron-rich and chromium-enriched, respectively. The transformation of ferrite to alpha and alpha prime is spinodal-like. In addition, abundant precipitation of G-phase was observed. These microstructural features are revealed in Fig. 13. The decomposition into alpha

and alpha prime has also been found recently after low temperature aging of types CF 8 and CF 8M steels [23]. These results indicate that the same low-temperature ferrite instability that has been documented for fully ferritic steels [24-29] is found in duplex steels containing small amounts of ferrite.

The results of the mechanical properties microprobe measurements are presented in Fig. 14. The ratio of post-aging hardness to the initial hardness is plotted against the aging time at 475°C. For aging times between 100 and 1000 hours, a 50% increase in hardness of the ferrite was found. For aging times beyond 1000 hours, a dramatic increase in hardness of approximately 400% was detected. Beyond an aging time 1000 hours, the hardness appears to remain constant.

Aging Behavior and Its Effect on Creep Properties

The beneficial effect of CRE additions on the creep properties of 308 steel welds has been known for some time but the basis for the improvement has not been clarified. Based on the present aging study, the most dramatic difference between the two alloy types following aging is the distribution of carbides. For both the homogenized and as-welded conditions, the type 308CRE alloy contained a relatively random distribution of precipitates after aging. In contrast, the distribution of carbides in the aged type 308 steel was very localized. Carbides form a continuous network along the austenite grain boundaries in the homogenized and aged material. A similar network of carbides is formed in the welded and aged alloy, although the carbides lie

along the initial ferrite/austenite interfaces in this material.
It was suggested that the absence of these carbide networks in
the type 308CRE alloy may be responsible for the improved creep
properties of 308CRE [13]. Examination of the fractured
specimens after creep testing has confirmed this hypothesis [30].
Representative micrographs of the fracture cross sections of
homogenized types 308 and 308CRE steels are shown in Fig. 15.
Prolific cracking in the region near the fracture is found in
type 308 steel, and this cracking is along the austenite grain
boundaries that are heavily lined with carbide precipitates. In
contrast, no significant cracking was found near the fracture in
the type 308CRE steel, in which precipitation along the austenite
grain boundaries was very limited. The role of the carbide
network in providing an easy path for crack formation explains
why cracks were previously found at the sigma/austenite
boundaries in the welded 308 steels and not at similar boundaries
in welded 308CRE [11]. The interconnected carbide network exists
only in the former alloy. However, when the observations of
abundant cracks were made, only optical microscopy was employed,
and the resolution was not sufficient to detect the presence or
absence of the carbide network in the welded materials.

Relationship Between Aging Behavior and 475°C Embrittlement

Mechanical properties microprobe hardness measurements
indicated that a significant increase in the ferrite hardness
occurred during low-temperature aging of duplex 308 welds. These
results suggest that such aging may lead to embrittlement.
Microstructural results show this potential embrittlement may be

due to a combination of ferrite decomposition into alpha and alpha prime as well as the precipitation of G-phase. The present results do not allow for a determination of the contribution each of these reactions has on the mechanical properties.

.Earlier results on ferritic steels have shown that embrittlement may occur after relatively short aging times [28,31]. The present hardness results confirm that a substantial increase in hardness (50%) is found after only 100 hours. However, the greatest effect occurs after 1000 hours. Previous studies did not extend significantly beyond ~1000 hours [28,31]. Since a hardness increase can be related to an increase in yield strength, and an increase in yield strength can, in turn, be associated with a degradation of impact properties, the present results imply that embrittlement may be much more severe after long term aging. Furthermore, if, in addition to the ferrite decomposition into alpha and alpha prime, the G-phase formation contributes to the embrittlement, then the apparent increased stability of G-phase in the type 308CRE steel may indicate that this alloy is more susceptible to embrittlement than the 308 steel. It is clear that this area requires additional work. Studies are presently underway at ORNL to examine the microstructural development as a function of aging time and temperature. In conjunction with further microprobe hardness testing, attempts will be to separate the effects of ferrite decomposition and G-phase formation.

CONCLUSIONS

The following conclusions can be drawn from this work:

1. The ferrite in type 308 and 308CRE steels is unstable and undergoes a transformation to sigma phase at aging temperatures between 550 and 850°C, whereas the ferrite decomposes into alpha and alpha prime at temperatures below 550°C.

2. Precipitation of carbides takes place during aging of type 308 steel, and the distribution of these precipitates is strongly dependent upon the initial condition of the alloy. In contrast, formation of titanium-rich precipitates in type 308CRE steel is more random throughout the structure and is basically independent of the initial condition.

3. The formation of a connected network of carbides in aged type 308 steel is the primary cause of the steel's inferior creep performance compared to the creep behavior of type 308CRE steel.

4. A significant increase in ferrite hardness was measured in low-temperature (<550°C) aged type 308 steel. This result indicates the residual ferrite in 308 welds may be subject to "475°C" embrittlement, and this embrittlement may be most severe for aging times of more than 1000 hours at 475°C. This potential embrittlement is due to a combination of ferrite decomposition into alpha and alpha prime, and precipitation of G-phase.

REFERENCES

1. J.C. Borland and R.N. Younger: Brit. Weld. J., 1960, vol. 7, pp.22-60.

2. F.C. Hull: Weld. J., 1967, vol. 46, pp. 399s-409s.

3. I. Masumoto, K. Tamaki, and M. Kutsuna: J. JWS, 1972, vol. 41, pp.1306-1314. Brutcher Trans. 8965/1973.

4. H. Thier: DVS-Berichte, 1975, vol. 33, pp. 69-75

5. Y. Arata, F. Matsuda, and S. Katayama: Trans. JWRI, 1976, vol. 5(2), pp. 35-51.

6. V. Kujanpää, N. Suutala, T. Takalo, and T. Moisio: Weld. Res. Int'l., 1979, vol. 9, pp. 55-76.

7. J.C. Lippold and W.F. Savage: Weld. J., 1982, vol. 61, pp. 388s-396s.

8. V.P. Kujanpää, S.A. David, and C.L. White: Weld. J., 1986, vol. 65, pp. 203s-212s.

9. N.C. Binkley, R.G. Berggren, and G.M. Goodwin: Weld. J., 1974, vol. 53, pp. 91s-95s.

10. R.T. King, J.O. Stiegler, and G.M. Goodwin: Weld. J., 1974, vol. 53, pp. 307s-313s.

11. J.O. Stiegler, R.T. King, and G.M. Goodwin: J. Eng. Mater. Technol., 1975, vol. 97, pp. 245-250.

12. D.P. Edmonds, Oak Ridge National Laboratory, Oak Ridge, TN 37831, unpublished results.

13. J.M. Vitek and S.A. David: Weld. J., 1984, vol. 63, pp. 246s-253s.

14. J.M. Vitek and S.A. David: Scripta Metall., 1985, vol. 19, pp. 23-26.

15. J.M. Vitek and S.A. David: Weld. J., 1986, vol. 65,

pp. 106s-111s.

16. J.M. Vitek: Metall. Trans. A, 1987, vol. 18A, pp. 154-156.

17. J.M. Vitek and S.A. David: Metall. Trans. A, 1987, in press.

18. S.A. David, J.M. Vitek, J.R. Keiser, and W.C. Oliver: Weld. J., accepted for publication.

19. AWS procedure A4.2-74, *Standard Procedures for Calibrating Magnetic Instruments to Measure the Delta Ferrite Content of Austenitic Stainless Steel Weld Metal*, American Welding Society, Miami, Fla., 1974

20. J.M. Vitek and R.L. Klueh: Metall. Trans. A, 1983, vol. 14A, pp. 1047-1055.

21. J.B. Pethica, R. Hutchings, and W.C. Oliver: Phil. Mag., 1983, vol. A48, p. 593.

22. W.C. Oliver, R. Hutchings, and J.B. Pethica: *Microindentation Techniques in Materials Science and Engineering*, ASTM STP 889, P.J. Blau and B.R. Lawn, eds., ASTM, Philadelphia, 1986, p. 90.

23. M.K. Miller and J. Bentley: J. de Physique, 1984, vol. 47-C7, pp. C7-239 - C7-244.

24. R.M. Fisher, E.J. Dulis, and K.G. Carroll: Trans. AIME, 1953, vol. 197, pp. 690-695.

25. R.O. Williams and H.W. Paxton: J. Iron Steel Inst., 1957, vol. 185, pp. 358-374.

26. D. Chandra and L.H. Schwartz: Metall. Trans. A, 1971, vol. 2A, p. 511.

27. J. Nishizawa, M. Hasebe, and M. Ko: Acta Metall., 1976, vol. 27, p. 817.

28. T.J. Nichol, A. Dotta, and G. Aggun: Metall. Trans. A, 1980,

vol. 11A, pp. 573-585.

29. S.S. Brenner, M.K. Miller, and W.A. Soffa: Scripta Metall., 1982, vol. 16, pp. 831-836.

30. J.M. Vitek, S.A. David, and V.K. Sikka: to be submitted to Weld. J. for publication.

31. P.J. Grobner: Metall. Trans. A, 1973, vol. 4A, pp. 251-260.

TABLE 1 - Major Constituents of Alloys Studied

Element	Homog. 308	Welded 308	Homog 308CRE	Welded 308CRE
Cr	20.9	20.2	20.0	19.8
Ni	10.3	9.4	10.0	9.9
Mn	1.6	1.7	2.0	2.0
Si	0.5	0.5	0.6	0.6
Ti	<0.01	<0.01	0.6	0.5
C	0.07	0.05	0.04	0.04
N_2	0.04	0.06	0.01	0.02

Figure Captions

Figure 1   Vertical section of the Fe-Cr-Ni ternary phase diagram
            at 70 wt % iron. The dashed line represents the
            approximate composition of type 308 stainless steel.

Figure 2   Creep rupture properties of GTA welds of large
            commercial heats of 308CRE tested at 650°C, and
            compared to creep-rupture properties of types 304 and
            308 GTA welds (taken from ref [12]).

Figure 3   Microstructures of (a,b) homogenized type 308 stainless
            steel (c,d) homogenized type 308CRE stainless steel.

Figure 4   As-welded microstructures of types (a) 308 and (b)
            308CRE stainless steels. Arrows point to ferrite
            phase.

Figure 5   (a) Carbide precipitation (arrowed) found along
            austenite grain boundaries in homogenized 308 steel
            aged at 650°C for 96 hours. (b) Carbide precipitation
            found along austenite/ferrite interface in welded 308
            steel aged at 650°C for 18 minutes.

Figure 6   Carbide precipitation along austenite/ferrite interface
            and G-phase precipitation within ferrite found in type
            308 stainless steel weld aged at 475°C for 4950 hours.

Figure 7   Random distribution of titanium-rich precipitates
            (arrows) in homogenized type 308CRE steel aged at 650°C
            for approximately 1000 hours.

Figure 8   G-phase precipitation along dislocations within the
            ferrite in homogenized type 308CRE steel aged at 650°C
            for 6 hours.

Figure 9   Amount of precipitate vs time for welded type 308
            stainless steel aged or creep tested at 650°C showing
            the lack of influence of stress on the precipitation
            behavior.

Figure 10   Similar to aged only specimens, precipitation behavior
            found in creep-tested type 308 stainless steel is along
            (a) austenite grain boundaries in the homogenized or
            (b) austenite/ferrite interfaces in the welded
            condition.

Figure 11   Decrease in ferrite content as a function of aging time
            at 650°C for welded types 308 and 308CRE steels.

Figure 12   Welded and creep tested (650°C/74 hours) type 308 steel
            showing dissolution of ferrite away from the initial
            austenite/ferrite interface, which is decorated by
            carbide precipitates.

Figure Captions (continued)

Figure 13 Electron micrograph of type 308 stainless steel welded and aged at 475°C for 4950 hours showing, under proper contrast conditions, the decomposition of ferrite as well as the abundant precipitation of G-phase.

Figure 14 Ratio of aged to as-welded hardness of ferrite in type 308 steel as a function of aging time at 475°C, showing an initial modest increase followed by a dramatic increase after 1000 hours.

Figure 15 Low magnification cross sections of ruptured (a) homogenized type 308, and (b) homogenized type 308CRE creep specimens tested at 650°C. (c) is an SEM micrograph of the fracture surface in (a) showing the presence of cracks (filled arrows) along the heavily precipitated austenite grain boundaries. Open arrows indicate some carbide networks where cracks did not form.
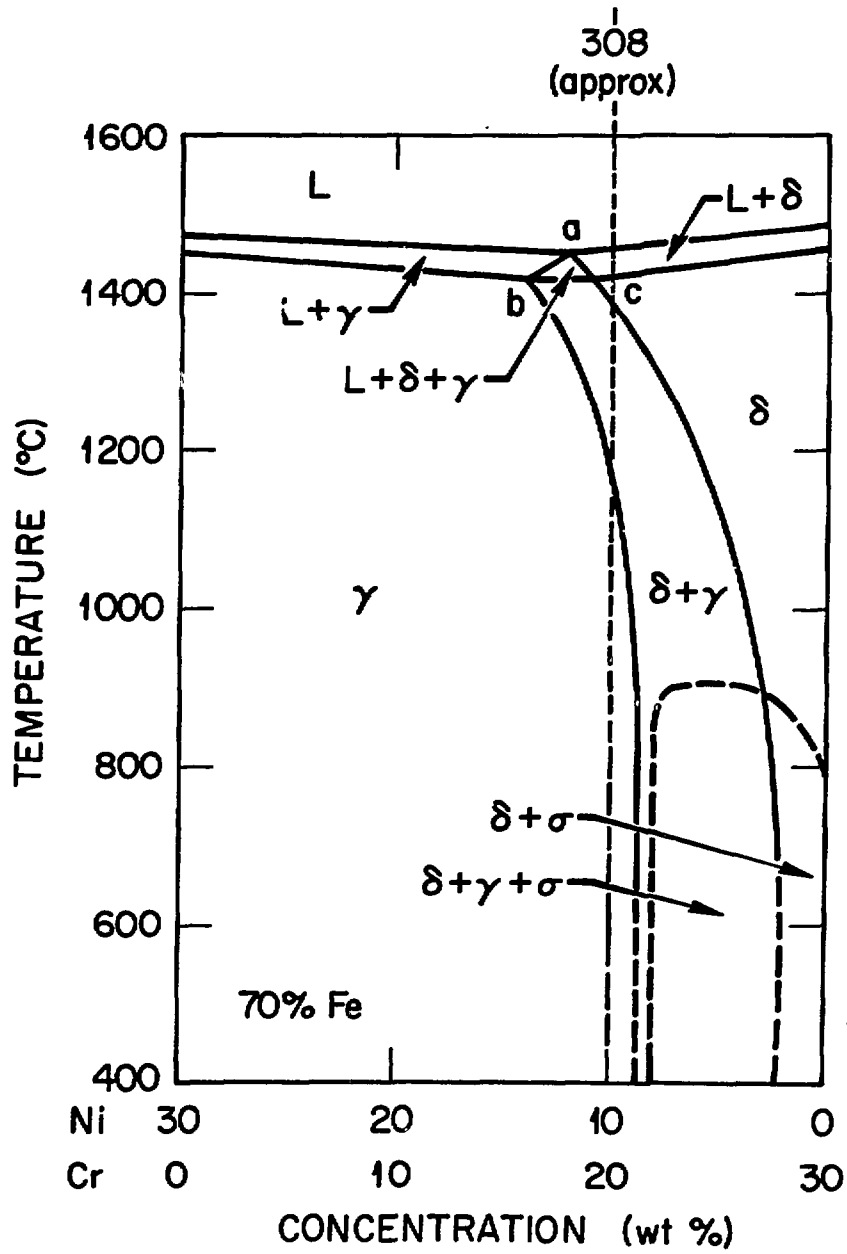
FIGURE 1
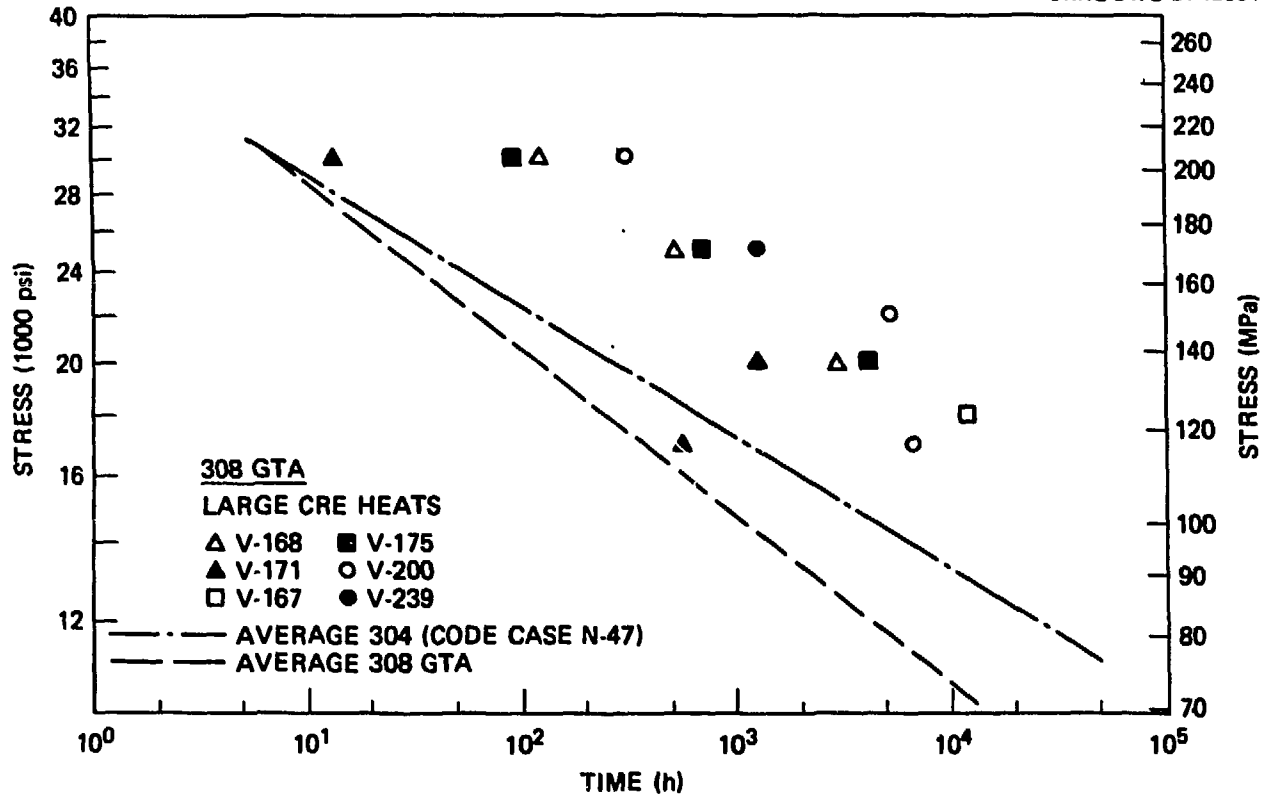
FIGURE 2

(a)
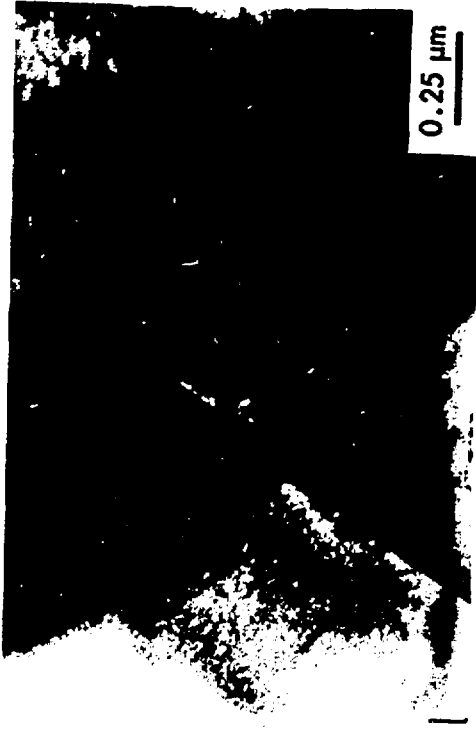
(b)
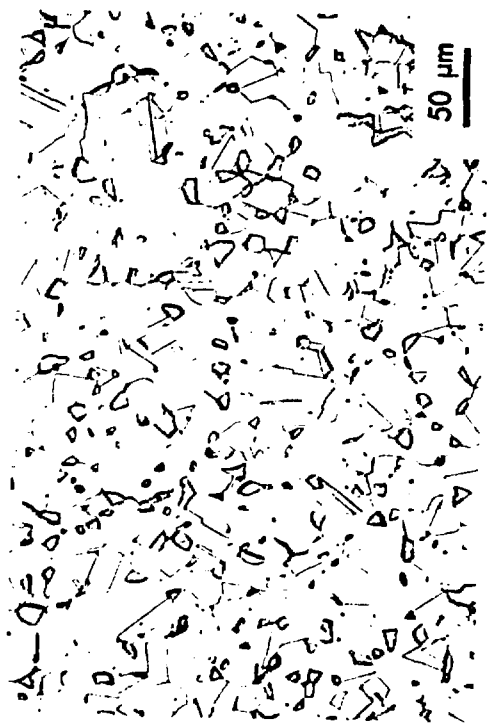
(c)

(d)

FIGURE 3

FIGURE 4

a

1.0 μm

b

FERRITE

0.5 μm

FIGURE 5

FIGURE 6

1 µm
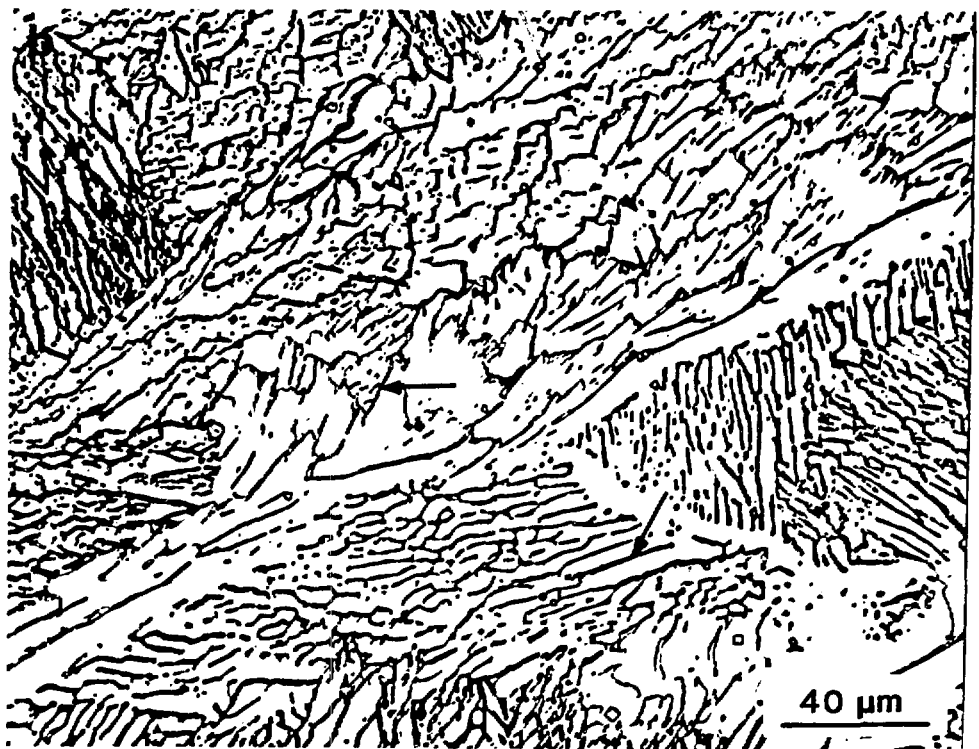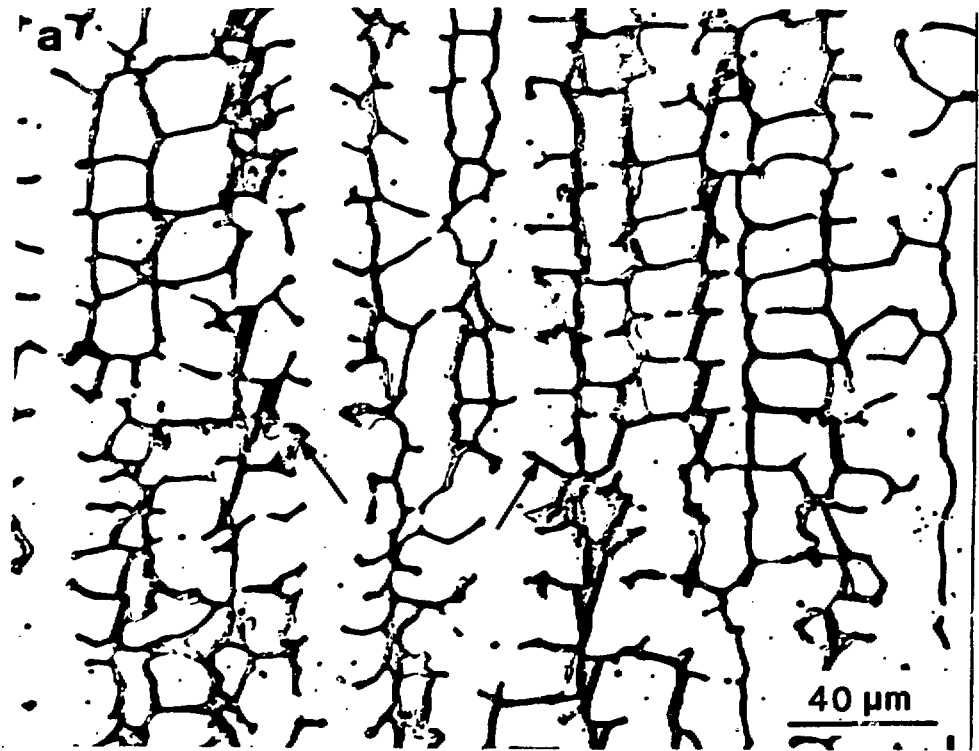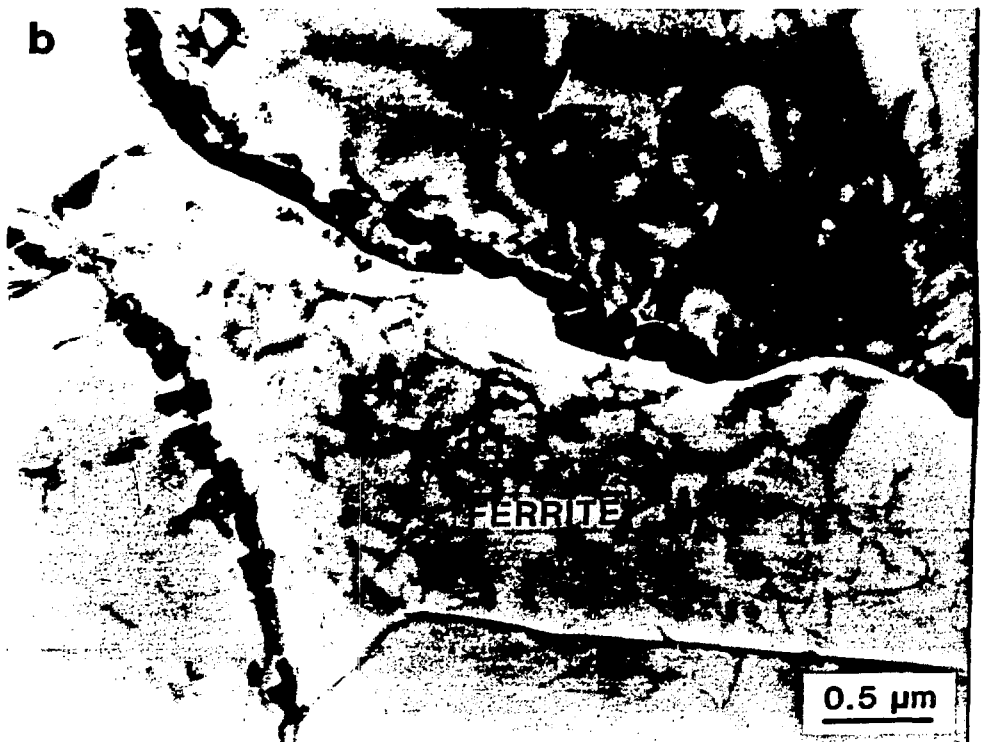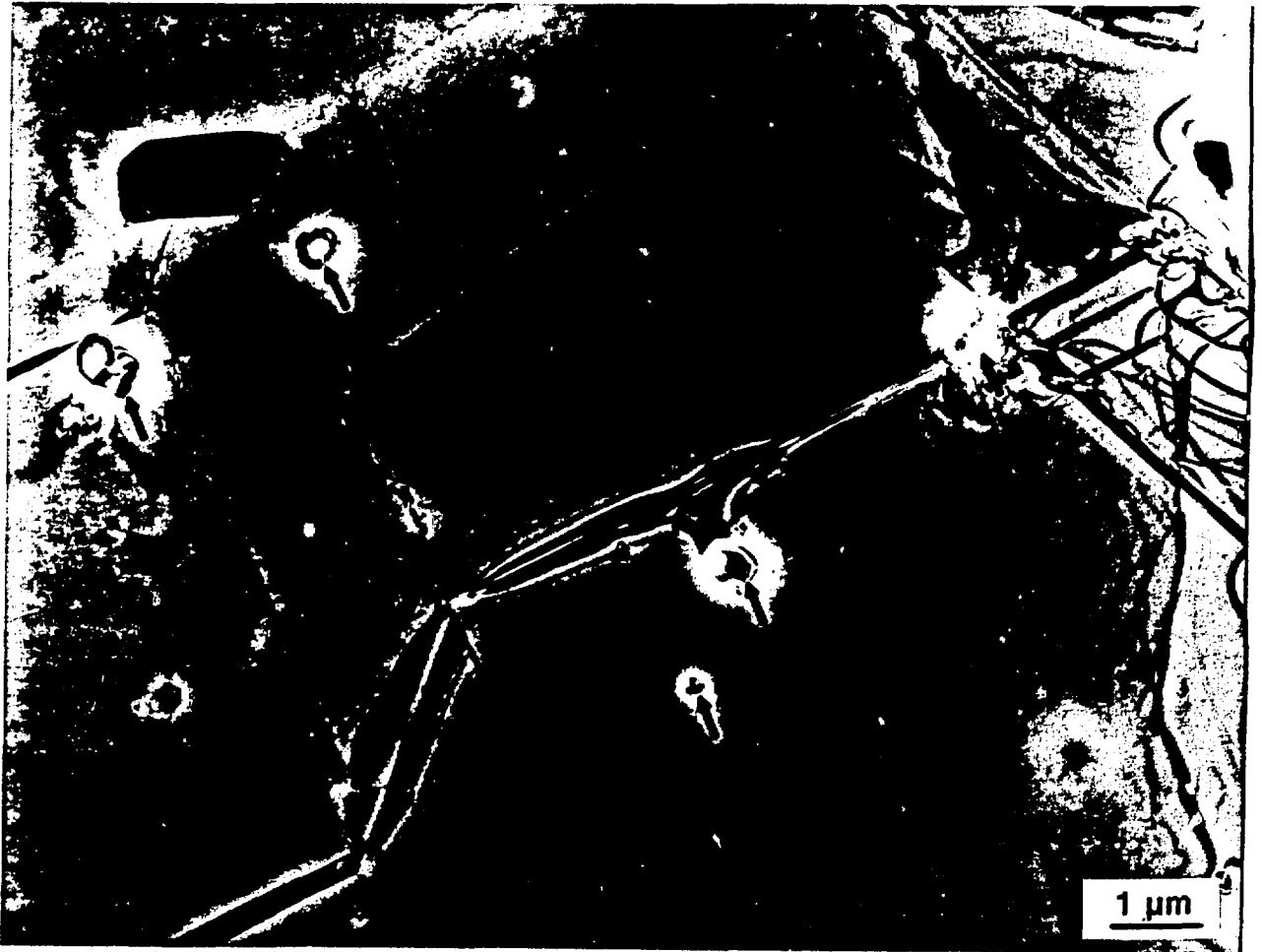
FIGURE 7

FIGURE 8

FIGURE 10
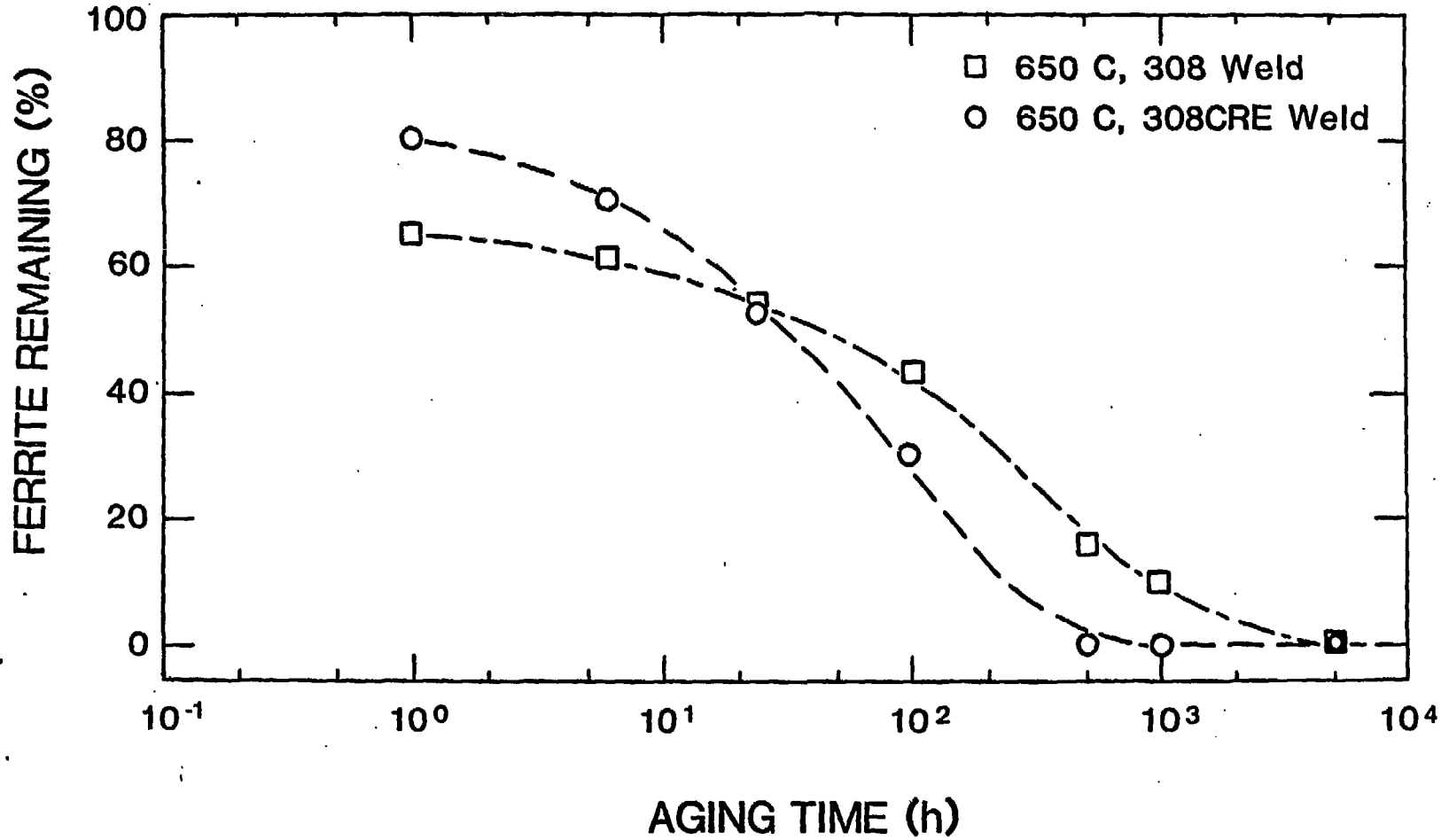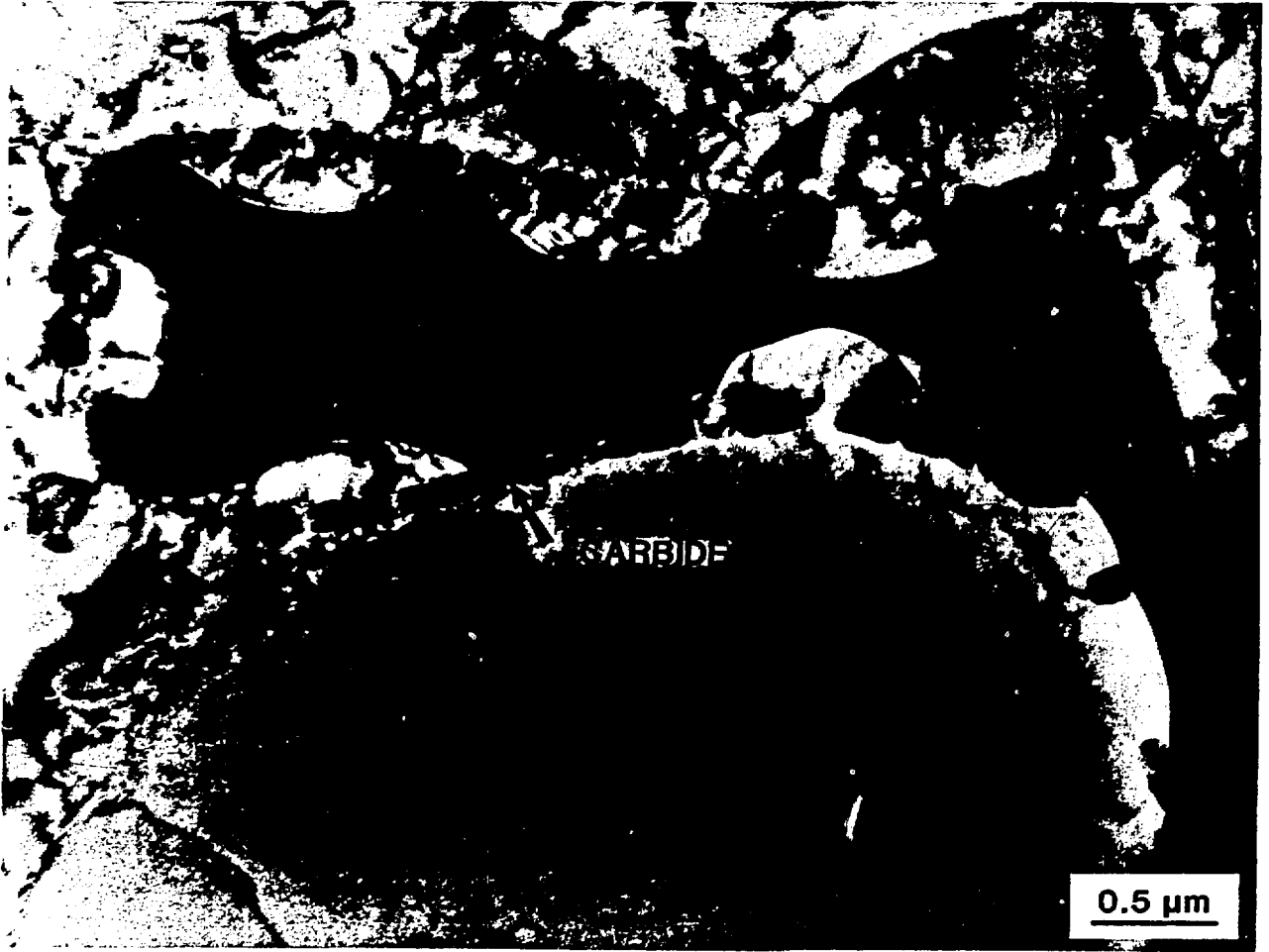
ORNL-DWG 87-13160

FIGURE 11

CARBIDE

0.5 μm

FIGURE 12

FIGURE 13
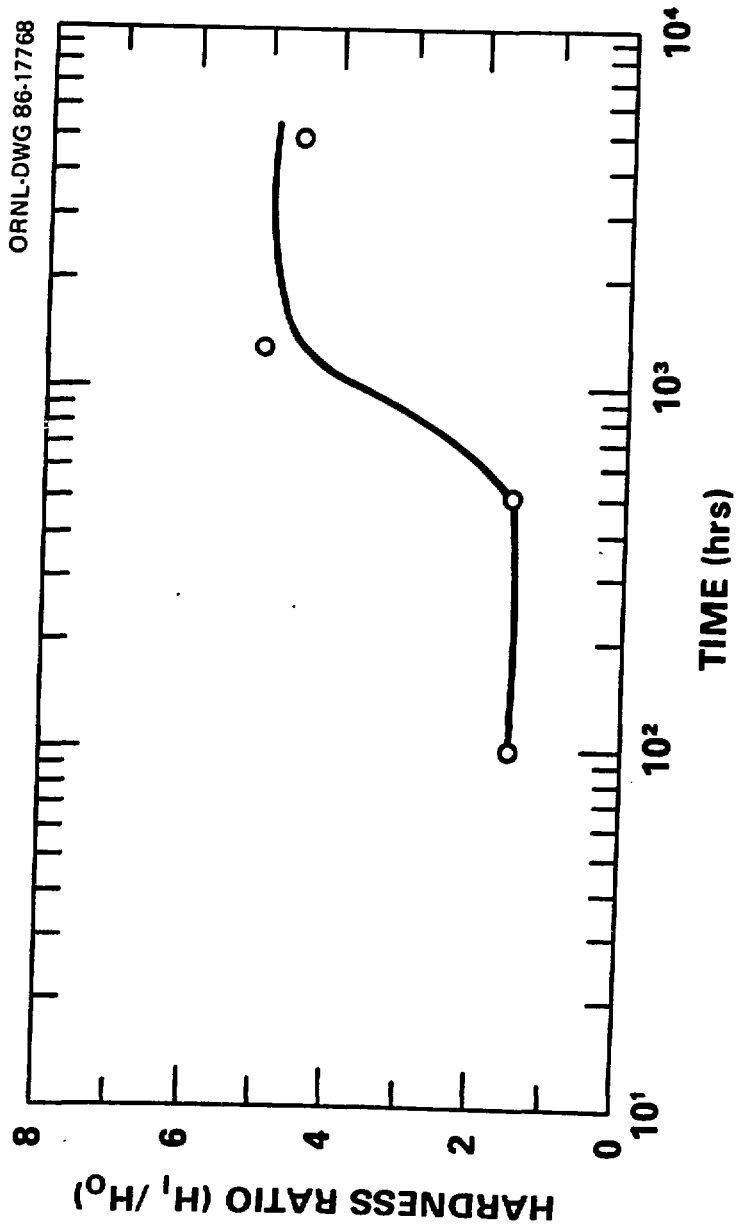
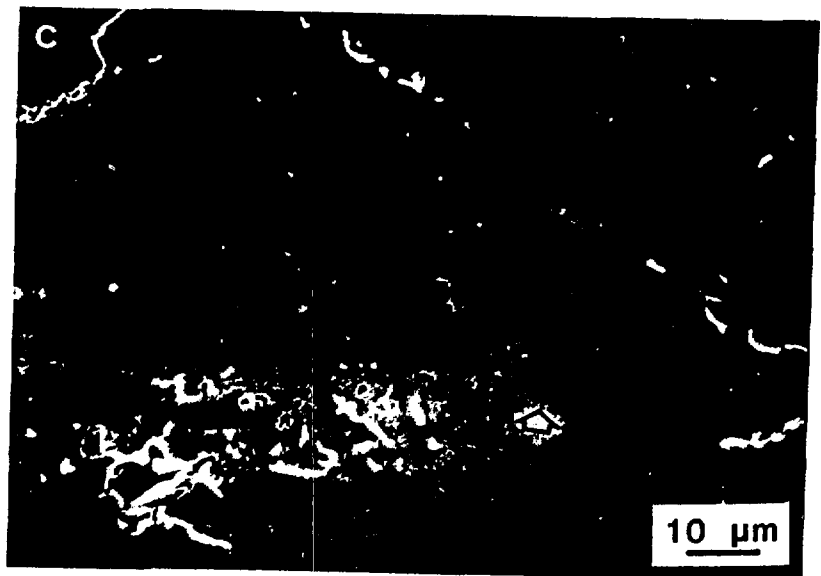ORNL-DWG 86-17768

HARDNESS RATIO (H_1/H_0)

TIME (hrs)
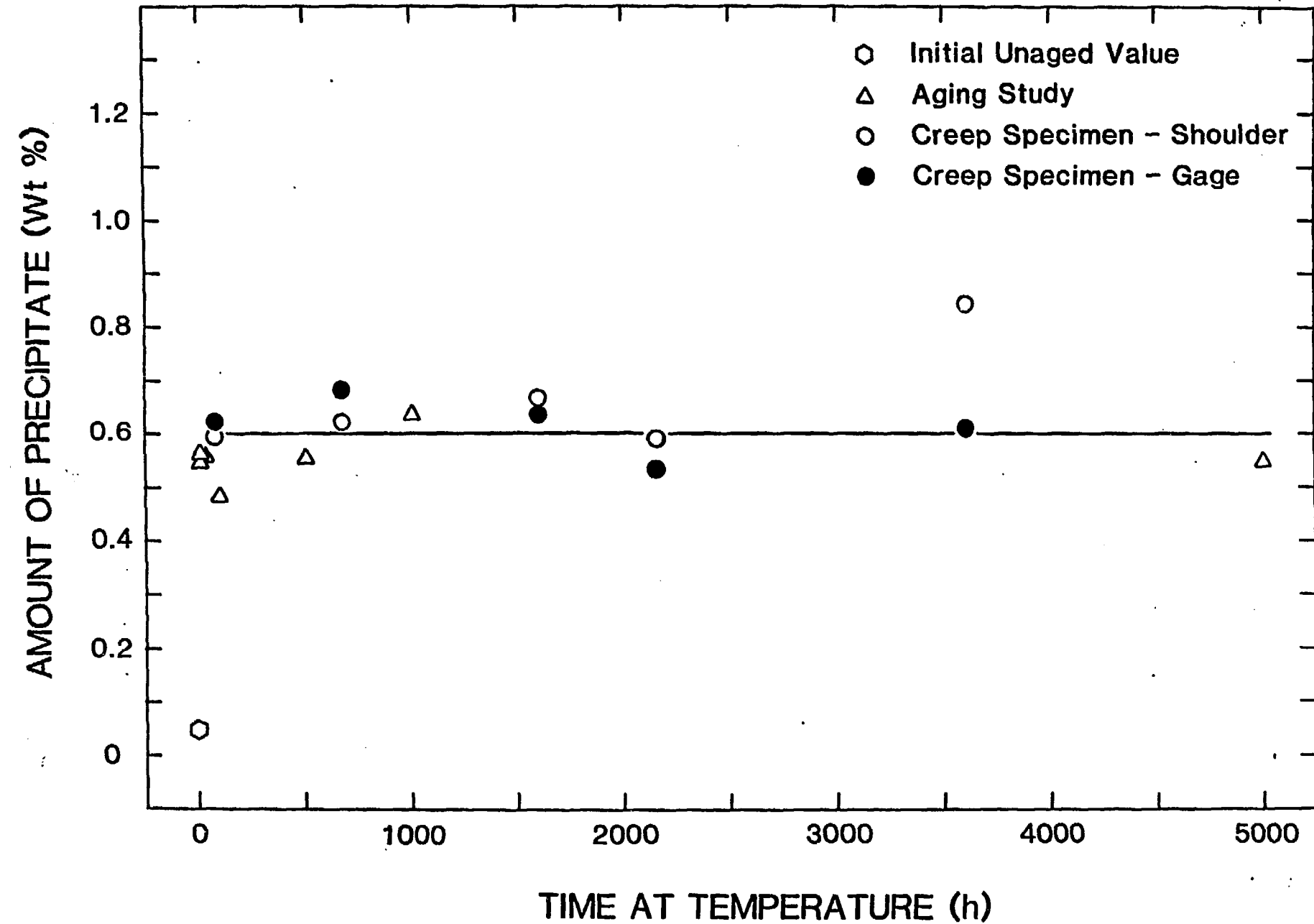
FIGURE 14
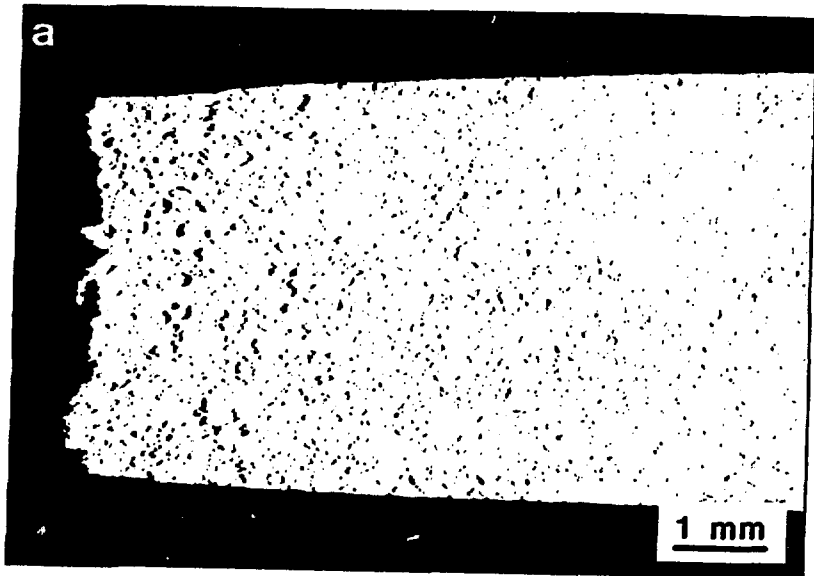
FIGURE 15

DISCLAIMER

This report was prepared as an account of work sponsored by an agency of the United States Government. Neither the United States Government nor any agency thereof, nor any of their employees, makes any warranty, express or implied, or assumes any legal liability or responsibility for the accuracy, completeness, or usefulness of any information, apparatus, product, or process disclosed, or represents that its use would not infringe privately owned rights. Reference herein to any specific commercial product, process, or service by trade name, trademark, manufacturer, or otherwise does not necessarily constitute or imply its endorsement, recommendation, or favoring by the United States Government or any agency thereof. The views and opinions of authors expressed herein do not necessarily state or reflect those of the United States Government or any agency thereof.